Check for updates

Cross Diffusion Effects on Chemically Reacting Magnetohydrodynamic Micropolar Fluid Between Concentric Cylinders

D. Srinivasacharya[1]
Department of Mathematics,
National Institute of Technology,
Warangal, Andhra Pradesh, 506004, India
e-mail: dsrinivasacharya@gmail.com;
dsc@nitw.ac.in

Mekonnen Shiferaw
Department of Mathematics,
Arba Minch University,
P. O. Box 72,
Arba Minch, Ethiopia
e-mail: mekk_aya@yahoo.com

The present study investigates magnetic, first-order chemical reaction, Soret and Dufour effects on electrically conducting micropolar fluid flow between two circular cylinders. The inner and outer surfaces of the annular cylinder are maintained at different constant wall temperature where the outer cylinder is rotating and inner cylinder remains stationary. The governing nonlinear partial differential equations are transformed into a system of ordinary differential equations (ODEs) using similarity transformations. The resulting equations are then solved for approximate analytical series solutions using homotopy analysis method (HAM). The effects of various parameters on the velocity, microrotation temperature and concentration are discussed and shown graphically. [DOI: 10.1115/1.4024838]

Keywords: heat and mass transfer, Soret effect, Dufour effect, micropolar fluid, magnetohydrodynamic (MHD), chemical reaction

1 Introduction

Convection heat transfer and fluid flow in an annulus between two vertical concentric cylinders have been the focus of investigation for many decades due to their wide range of practical applications such as electrical machineries where heat transfer occurs in the annular gap between the rotor and stator, growth of single silicon crystals, heat exchangers, cooling systems for electronic devices, solar collectors and other rotating systems [1,2]. The effect of rotating the inner cylinder for a concentric annulus was first studied by Taylor [3]. According to the Taylor-Couette theory, the flow of a fluid takes place in the gap between two concentric cylinders as a result of rotation of one or both of them. Fusegi et al. [4] studied mixed convection flows within a horizontal concentric annulus with a heated rotating inner cylinder. Kataoka [5] analyzed the flow of Newtonian fluid between concentric cylinders where the inner cylinder was rotated at a constant speed and the outer cylinder was stationary. El-Shaarawi and Khamis [6] numerically examined the induced flow in uniformly heated vertical annuli with rotating inner walls. Kou and Huang [7] solved the problem of fully developed laminar mixed convection through a vertical annular duct embedded in a porous medium.

A large amount of research work has been reported in the field of mathematical model for chemical reaction analysis. The study of heat and mass transfer with chemical reaction is of considerable importance in chemical and hydrometallurgical industries. For example, formation of smog is a first-order homogeneous chemical reaction. Considering the emission of NO_2 from automobiles and other smoke-stacks, NO_2 reacts chemically in the atmosphere with unburned hydrocarbons (aided by sunlight) and produces peroxyacetyl nitrate, which forms an envelope can be termed as photochemical smog. Kermlt et al. [8] reported experimental results about mass transfer in concentric rotating cylinders with surface chemical reaction in the presence of Taylor vortexes. Pop et al. [9] investigated the steady fully developed mixed convection flow in a vertical channel with first-order chemical reaction. Shateyi et al. [10] considered the two-dimensional flow of an incompressible viscous fluid through a nonporous channel with heat generation and a chemical reaction.

When heat and mass transfer occur simultaneously in a moving fluid, the relations between the fluxes and the driving potentials are of a more intricate nature. It has been observed that an energy flux can be generated not only by temperature gradients but also by concentration gradients. The energy flux caused by a concentration gradient is termed the diffusion-thermo (Dufour) effect. On the other hand, mass fluxes can also be created by temperature gradients and this embodies the thermal-diffusion (Soret) effect. In most of the studies related to heat and mass transfer process, Soret and Dufour effects are neglected on the basis that they are of a smaller order of magnitude than the effects described by Fouriers and Ficks laws. But these effects are considered as second order phenomena and may become significant in areas such as hydrology, petrology, geosciences, etc. Soret and Dufour effects are important for intermediate molecular weight gases in coupled heat and mass transfer in binary systems, often encountered in chemical process engineering and also in high-speed aerodynamics. Soret and Dufour effects are also critical in various flow regimes occurring in chemical and geophysical systems. Kafoussias et al. [11] investigated Dufour and Soret effects on mixed free forced convective and mass transfer boundary layer flow with temperature dependent viscosity. Awad and Sibanda [12] examined Dufour and Soret effects on heat and mass transfer in a micropolar fluid in a horizontal channel. Sudarsan Reddy et al. [13] obtained the finite element analysis of thermodiffusion and diffusion- thermo effects on convective heat and mass transfer flow through a porous medium in cylindrical annulus in the presence of constant heat source, but they considered annulus without rotation. Recently, finite element analysis of thermodiffusion effect on convective heat and mass transfer through a porous medium in a circular annulus has been presented by Sulochana et al. [14].

In recent years, progress has been considerably made in the study of magnetohydrodynamic (MHD) flow and heat transfer due to the effect of magnetic fields on the boundary layer flow control

[1]Corresponding author.

Contributed by the Heat Transfer Division of ASME for publication in the Journal of Heat Transfer. Manuscript received May 28, 2012; final manuscript received June 4, 2013; published online October 14, 2013. Assoc. Editor: William P. Klinzing.

 Copyright © 2013 by ASME

Downloaded from http://asmedigitalcollection.asme.org/heattransfer/article-pdf/135/12/122003/6204608/ht_135_12_122003.pdf by National Institute of Technology- Warngal user on 08 January 2025

and on the performance of many systems using electrically conducting fluids. In addition, this type of flow finds applications in many engineering problems such as MHD generators, plasma studies, nuclear reactors, and geothermal energy extractions, boundary layer control in the field of aerodynamics, in rocket propulsion control, crystal growth technology, astrophysical plasma fluid dynamics. Magnetohydrodynamic equations are ordinary electromagnetic and hydrodynamic equations modified to take into account the interaction between the motion of the fluid and the electromagnetic field. Takhar et al. [15] numerically investigated the MHD stability problem for dissipative Couette flow in a narrow gap. Panja et al. [16] studied hydromagnetic flow of Reiner-Rivlin fluid between two coaxial circular cylinders with porous walls. KunugiLi and Serizawa [17] presented numerical solutions of MHD effect on flow structures and heat transfer characteristics of liquid metal-gas annular flow in a vertical pipe considering a transverse magnetic field. Siddiqa et al. [18] considered double diffusive magnetoconvection fluid flow in a strong cross magnetic field with uniform surface heat and mass flux.

It is well known that most fluids which are encountered in chemical and allied processing applications do not satisfy the classical Newton's law and are accordingly known as non-Newtonian fluids. The study of non-Newtonian fluid flows has gained much attention from the researchers because of its applications in biology, physiology, technology and industry. In addition, the effects of heat and mass transfer in non-Newtonian fluid also have great importance in engineering applications; for instance, the thermal design of industrial equipment dealing with molten plastics, polymeric liquids, foodstuffs, or slurries. A number of mathematical models have been proposed to explain the rheological behavior of non-Newtonian fluids. Further, there exist several approaches to study the mechanics of fluids with a substructure. Ericson [19,20] derived field equations which account for the presence of substructures in the fluid. Eringen [21] first formulated the theory of micropolar fluids which display the effects of local rotary inertia and couple stresses. This theory can be used to explain the flow of colloidal fluids, liquid crystal, animal blood, etc. Physically, micropolar fluids may be described as non-Newtonian fluids consisting of dumb-bell molecules or short rigid cylindrical element, polymer fluids, fluid suspension, etc. The presence of dust or smoke, particularly in a gas, may also be modeled using micropolar fluid dynamics.

The HAM [22] was first proposed by Liao in 1992, is one of the most efficient methods in solving different types of nonlinear equations such as coupled, decoupled, homogeneous and nonhomogeneous. Also, HAM provides us a great freedom to choose different base functions to express solutions of a nonlinear problem [23]. The application of HAM in engineering problems is highly considered by scientists, because it provides with us a convenient way to control the convergence of approximation series, which is a fundamental qualitative difference in analysis between HAM and other methods. Later Liao [24] presented an optimal homotopy analysis approach for strongly nonlinear differential equations. HAM is used to get analytic approximate solutions for heat transfer of a micropolar fluid through a porous medium with radiation by Rashidi et al. [25]. Si et al. [26] accessed HAM solutions for the asymmetric laminar flow in a porous channel with expanding or contracting walls.

The objective of the present work is to study convective heat and mass transfer of a MHD micropolar fluid flow between concentric cylinders with thermal-diffusion, diffusion-thermo, and chemical reaction effects in the presence of applied magnetic field. The governing nonlinear differential equations have been solved by using HAM. The convergent region of the HAM solution for the model is introduced graphically and examined. The velocity, microrotation, temperature, and concentration functions variations are shown graphically for various values of parameters.

2 Mathematical Formulation

Consider a steady, laminar, incompressible micropolar fluid in an annulus between infinite vertical concentric circular cylinders of radii a and b $(a < b)$. Choose the cylindrical polar coordinate system (r, φ, z) with z-axis as the common axis for both cylinders. The inner cylinder is at rest and the outer cylinder is rotating with constant angular velocity Ω. The flow being generated due to the rotation of the outer cylinder. Since the flow is fully developed and the cylinders are of infinite length, the flow depends only on r. The outer cylinder is maintained at a uniform temperature T_b and the inner cylinder at a temperature T_a. The flow is subjected to a uniform magnetic field along the radial direction and no external electric field is applied. Assume that the magnetic Reynolds number is very small so that the induced magnetic field can be neglected in comparison with the applied magnetic field. Further, assume that all the fluid properties are constant except the density in the buoyancy term of the balance of momentum equation. In addition, the Soret and Dufour effects with chemical reaction are considered. With the above assumptions and Boussinesq approximations with energy and concentration, the equations governing the steady flow of an incompressible micropolar fluid [27,28], under usual MHD approximations are

$$\frac{\partial u}{\partial \varphi} = 0 \tag{1}$$

$$\frac{\partial p}{\partial r} = \frac{\rho u^2}{r} - \sigma B_0^2 u \tag{2}$$

$$-\kappa\frac{\partial \Gamma}{\partial r} + (\mu+\kappa)\left(\frac{1}{r}\frac{\partial u}{\partial r} - \frac{u}{r^2} + \frac{\partial^2 u}{\partial r^2}\right) + \rho g^*(\beta_T(T-T_0) + \beta_c(C-C_0)) - \sigma B_0^2 u = 0 \tag{3}$$

$$-2\kappa\Gamma + \kappa\left(\frac{\partial u}{\partial r} + \frac{u}{r}\right) + \gamma\left(\frac{1}{r}\frac{\partial \Gamma}{\partial r} + \frac{\partial^2 \Gamma}{\partial r^2}\right) = 0 \tag{4}$$

$$\alpha\left(\frac{1}{r}\frac{\partial T}{\partial r} + \frac{\partial^2 T}{\partial r^2}\right) + 2\kappa\left(\frac{1}{2r}\frac{\partial (ru)}{\partial r} - \Gamma\right)^2 + (\mu+\kappa)\left(\frac{\partial u}{\partial r} - \frac{u}{r}\right)^2 + \gamma\left(\frac{\partial \Gamma}{\partial r}\right)^2 + \frac{D_m K_T}{C_s C_p}\left(\frac{1}{r}\frac{\partial C}{\partial r} + \frac{\partial^2 C}{\partial r^2}\right) = 0 \tag{5}$$

$$D_m\left[\frac{\partial^2 C}{\partial r^2} + \frac{1}{r}\frac{\partial C}{\partial r}\right] + \frac{D_m K_T}{T_m}\left[\frac{\partial^2 T}{\partial r^2} + \frac{1}{r}\frac{\partial T}{\partial r}\right] - k_1(C - C_a) = 0 \tag{6}$$

where u is velocity in φ direction Γ is microrotaion, T is the temperature, C is the concentration, ρ fluid density, μ dynamic coefficient of viscosity, κ is vortex viscosity, γ is the spin gradient viscosity, g^* is the acceleration due to gravity, β_T is the coefficient of thermal expansion, β_c is the coefficient of solutal expansion, α is the thermal diffusivity, D_m is the mass diffusivity, C_p is the specific heat capacity, C_s is the concentration susceptibility, and T_m is the mean fluid temperature, k_1 is the rate of chemical reaction parameter, B_0 magnetic induction and σ is electric conductivity of the fluid.

The boundary conditions are

$$u = 0, \quad \Gamma = 0, \quad T = T_a, \quad C = C_a, \quad \text{at} \quad r = a \tag{7a}$$

$$u = b\Omega, \quad \Gamma = \frac{1}{2r}\frac{\partial}{\partial r}(ru), \quad T = T_b, \quad C = C_b, \quad \text{at} \quad r = b \tag{7b}$$

Introducing the following transformations

$$r = b\sqrt{\lambda}, \quad u = \frac{\Omega}{\sqrt{\lambda}} f(\lambda), \quad \Gamma = \frac{\Omega}{b} g(\lambda), \quad T - T_a = (T_b - T_a)\theta(\lambda), \quad C - C_a = (C_b - C_a)\phi(\lambda) \tag{8}$$

in Eqs. (3)–(6), we get the following dimensionless equations:

Downloaded from http://asmedigitalcollection.asme.org/heattransfer/article-pdf/135/12/122003/6204608/ht_135_12_122003.pdf by National Institute of Technology- Warngal user on 08 January 2025

$$-\frac{2N}{1-N}\lambda g' + \frac{4}{1-N}f'' + \sqrt{\lambda}(g_s\theta + g_c\phi) - H_a^2 f = 0 \quad (9)$$

$$-g + f' + \frac{2(2-N)}{m^2}(g' + \lambda g'') = 0 \quad (10)$$

$$(\lambda^3\theta'' + \lambda^2\theta') + \frac{\mathrm{Br}}{1-N}\left[(N/2)\lambda^2(f'-g)^2 + (f-\lambda f')^2 + \frac{N(2-N)}{m^2}\lambda^3 g'^2\right] + D_f P_r(\lambda^3\phi'' + \lambda^2\phi') = 0 \quad (11)$$

$$\frac{1}{S_c}(\lambda\phi'' + \phi') + S_r(\lambda\theta'' + \theta') - \frac{K}{4}\phi = 0 \quad (12)$$

where primes denote differentiation with respect to the variable λ, $N = \kappa/(\mu+\kappa)$ is coupling number, $\mathrm{Re} = \rho\Omega b/\mu$ is the Reynolds number, $\mathrm{Pr} = \mu C_p/K_T$ is the Prandtl number, $\mathrm{Gr_T} = (g\beta_T(T_b - T_a)b^3/\nu^2)$ is the temperature Grashof number, $\mathrm{Gr_C} = (g\beta_C(C_b - C_a)b^3/\nu^2)$ is the mass Grashof number, $H_a^2 = \sigma B_0^2 b^2/\mu$ is Hartman number, υ is kinematic viscosity, $B_r = (\Omega^2\mu/\alpha(T_b - T_a))$ is the Brinkman number, $m^2 = (b^2\kappa(2\mu+\kappa)/\gamma(\mu+\kappa))$ is micropolar parameter, $D_f = (D_m K_T(C_b - C_a)/\upsilon C_s C_p(T_b - T_a))$ is the Dufour number, $S_c = \nu/D_m$ is the Schmidt number, $S_r = (D_m K_T(T_b - T_a)/\upsilon T_m(C_b - C_a))$ is the Soret number and $K = k_1 b^2/\upsilon$ chemical reaction parameter. $g_s = G_r/\mathrm{Re}$ is the temperature buoyancy parameter, $g_c = G_c/\mathrm{Re}$ is the mass buoyancy parameter.

The corresponding boundary conditions in dimensionless form are

$$f(\lambda_0) = 0, \quad g(\lambda_0) = 0, \quad \theta(\lambda_0) = 0, \quad \phi(\lambda_0) = 0, \quad \text{where} \quad \lambda_0 = \frac{a}{b} \quad (13a)$$

$$f(1) = b, \quad g(1) = \left[\frac{df}{d\lambda}\right]_{\lambda=1}, \quad \theta(1) = 1, \quad \phi(1) = 1 \quad (13b)$$

3 The HAM Solution of the Problem

The solution to the system of nonlinear ordinary differential equations (9)–(12) is obtained by using the analytical technique HAM. It has been successfully applied to many nonlinear problems such as boundary layer flows, heat transfer, MHD flows of non-Newtonian fluids and many others. The basic idea behind the use of the homotopy analysis method is the replacement of a nonlinear equation by a system of ODEs that can easily be solved with the help of symbolic computation software. The solution of this system of ODEs is used to form a convergent series which is the solution of the original nonlinear equation. A detailed explanation of the method is given in the book by Liao [22]. In using the HAM, and in order to effectively control the region and the rate of convergence of the HAM series solution, one has to carefully select an initial approximation, an auxiliary linear operator, an auxiliary function and a convergence controlling auxiliary parameter. Suggestions on how to select this combination of parameters are given in Ref. [29] for general nonlinear problems.

For the analytical solution of Eqs. (9)–(12) using HAM, we choose the initial approximations of $f(\lambda), g(\lambda), \theta(\lambda)$ and $\phi(\lambda)$ as

$$f_0(\lambda) = b\frac{(\lambda-\lambda_0)}{1-\lambda_0}, \quad g_0(\lambda) = \frac{\lambda-\lambda_0}{(1-\lambda_0)^2}, \quad \theta_0(\lambda) = \frac{\lambda-\lambda_0}{1-\lambda_0}, \quad \phi_0(\lambda) = \frac{\lambda-\lambda_0}{1-\lambda_0} \quad (14)$$

and choose the auxiliary linear operators $L = \partial^2/\partial\lambda^2$ with the property $L(c_1 + c_2\lambda) = 0$, where c_1 and c_2 are constants.

The zeroth-order deformation equation is given by

$$(1-p)L[f(\lambda;p) - f_0(\lambda)] = ph_1N_1[f(\lambda,p)], \quad (1-p)L[g(\eta;p) - g_0(\lambda)] = ph_2N_2[g(\lambda,p)] \quad (15a)$$

$$(1-p)L[\lambda(\lambda;p) - \theta_0(\lambda)] = ph_3N_3[\theta(\lambda,p)], \quad (1-p)L[\phi(\lambda;p) - \phi_0(\lambda)] = ph_4N_4[\phi(\lambda,p)] \quad (15b)$$

where h_1, h_2, h_3, and h_4 are nonzero auxiliary parameters and $p \in [0,1]$ is the embedding parameter. Accordingly the boundary conditions are given by

$$f(\lambda_0;p) = 0, \quad g(\lambda_0;p) = 0, \quad \theta(\lambda_0;p) = 0, \quad \phi(\lambda_0;p) = 0$$
$$f(1;p) = b, \quad g(1;p) = \frac{d}{d\lambda}[f(1;p)], \quad \theta(1;p) = 1, \quad \phi(1;p) = 1 \quad (16)$$

The nonlinear operators N_1, N_2, N_3, and N_4 are defined as

$$N_1[f(\lambda,p)] = -\frac{2N}{1-N}\lambda g' + \frac{4}{1-N}f'' + \sqrt{\lambda}(g_s\theta + g_c\phi) - H_a^2 f \quad (17a)$$

$$N_2[g(\lambda,p)] = -g + f' + \frac{2(2-N)}{m^2}(g' + \lambda g'') \quad (17b)$$

$$N_3[\theta(\lambda,p)] = (\lambda^3\theta'' + \lambda^2\theta') + \frac{\mathrm{Br}}{1-N} \times \left[(N/2)\lambda^2(f'-g)^2 + (f-\lambda f')^2 + \frac{N(2-N)}{m^2}\lambda^3 g'^2\right] + D_f P_r(\lambda^3\phi'' + \lambda^2\phi') \quad (17c)$$

$$N_4[\phi(\lambda,p)] = \frac{1}{S_c}(\lambda\phi'' + \phi') + S_r(\lambda\theta'' + \theta') - \frac{K}{4}\phi \quad (17d)$$

If $p = 0$, the above deformation equation will give the initial approximations

$$f(\lambda;0) = f_0(\lambda), \quad g(\lambda;0) = g_0(\lambda), \quad \theta(\lambda;0) = \theta_0(\lambda), \quad \phi(\lambda;0) = \phi_0(\lambda) \quad (18)$$

and when $p = 1$, Eqs. (15) are same as Eqs (9)–(12), respectively; therefore, at $p = 1$, we get the final solutions

$$f(\lambda;1) = f(\lambda), \quad g(\lambda;1) = g(\lambda), \quad \theta(\lambda;1) = \theta(\lambda), \quad \phi(\lambda;1) = \phi(\lambda) \quad (19)$$

If the embedding parameter p increases from 0 to 1 then $f(\lambda;p), g(\lambda;p), \theta(\lambda;p)$, and $\phi(\lambda;p)$ varying continuously from the initial guesses $f_0(\lambda), g_0(\lambda), \theta_0(\lambda)$, and $\phi_0(\lambda)$ to the final solution $f(\lambda), g(\lambda), \theta(\lambda)$, and $\phi(\lambda)$ which are called the zeroth-order deformation equation. This continuous variation from the initial guess to the exact solution as q going from 0 to 1 is called deformation in topology.

Next, the mth-order deformation equations follow as

$$L[f_m(\eta) - \chi_m f_{m-1}(\lambda)] = h_1 R_m^f(\lambda), \quad L[g_m(\lambda) - \chi_m g_{m-1}(\lambda)] = h_2 R_m^g(\lambda)$$
$$L[\theta_m(\lambda) - \chi_m \theta_{m-1}(\lambda)] = h_3 R_m^\theta(\lambda), \quad L[\phi_m(\lambda) - \chi_m \phi_{m-1}(\lambda)] = h_4 R_m^\phi(\lambda) \quad (20)$$

with the boundary conditions

$$f_m(0) = 0, \quad f_m(1) = 0, \quad g_m(0) = 0, \quad g_m(1) = 0, \quad \theta_m(0) = 0, \quad \theta_m(1) = 0, \quad \phi_m(0) = 0, \quad \phi_m(1) = 0 \quad (21)$$

where

Downloaded from http://asmedigitalcollection.asme.org/heattransfer/article-pdf/135/12/122003/6204608/ht_135_12_122003.pdf by National Institute of Technology- Warngal user on 08 January 2025

$$R^f_{\mathrm{m}}(\lambda) = -\frac{2N}{1-N}\lambda g'_{\mathrm{m}-1} + \frac{4}{1-N}f''_{\mathrm{m}-1} + \sqrt{\lambda}(g_s\theta_{\mathrm{m}-1} + g_c\phi_{\mathrm{m}-1}) - H_a^2 f_{\mathrm{m}-1} \tag{22a}$$

$$R^g_{\mathrm{m}}(g) = -g_{\mathrm{m}-1} + f'_{\mathrm{m}-1} + \frac{2(2-N)}{m^2}(g'_{\mathrm{m}-1} + \lambda g''_{\mathrm{m}-1}) \tag{22b}$$

$$R^\theta_{\mathrm{m}}(\lambda) = (\lambda^3\theta''_{\mathrm{m}-1} + \lambda^2\theta'_{\mathrm{m}-1}) + \frac{Br}{1-N} \times \left[(N/2)\lambda^2\sum_{n=0}^{m-1}(f'_{\mathrm{m}-1-n}f'_n - 2f_{\mathrm{m}-1-n}g_n + g_{\mathrm{m}-1-n}g_n) + \sum_{n=0}^{m-1}(f_{\mathrm{m}-1-n}f_n - 2\lambda f_n f'_{\mathrm{m}-1-n} - \lambda^2 f'_{\mathrm{m}-1-n}f'_n) + \frac{N(2-N)}{m^2}\lambda^3\sum_{n=0}^{m-1}g'_{\mathrm{m}-1-n}g'_n\right] + D_{\mathrm{f}}P_{\mathrm{r}}(\lambda^3\phi''_{\mathrm{m}-1} + \lambda^2\phi'_{\mathrm{m}-1}) \tag{22c}$$

$$R^\phi_{\mathrm{m}}(\lambda) = \frac{1}{S_{\mathrm{c}}}(\lambda\phi''_{\mathrm{m}-1} + \phi'_{\mathrm{m}-1}) + S_r(\lambda\theta''_{\mathrm{m}-1} + \theta'_{\mathrm{m}-1}) - \frac{K}{4}\phi_{\mathrm{m}-1} \tag{22d}$$

for m being integer and

$$\chi_{\mathrm{m}} = 0 \quad \text{for} \quad m \le 1 \qquad = 1 \quad \text{for} \quad m > 1 \tag{23}$$

The initial guess approximations $f_0(\lambda), g_0(\lambda), \theta_0(\lambda)$, and $\phi_0(\lambda)$, the linear operator L and the auxiliary parameters h_1, h_2, h_3, and h_4 are assumed to be selected such that Eqs. (15) and (16) have solution at each point $p \in [0, 1]$ and also with the help of Taylor's series and due to Eq. (18); $f(\lambda;p), g(\lambda;p), \theta(\lambda;p)$, and $\phi(\lambda;p)$ can be expressed in series of q as

$$f(\lambda;p) = f_0(\lambda) + \sum_{\mathrm{m}=1}^{\infty} f_{\mathrm{m}}(\lambda)p^m, \quad g(\lambda;p) = g_0(\lambda) + \sum_{\mathrm{m}=1}^{\infty} g_{\mathrm{m}}(\lambda)p^m$$
$$\theta(\lambda;p) = \theta_0(\lambda) + \sum_{\mathrm{m}=1}^{\infty} \theta_{\mathrm{m}}(\lambda)p^m, \quad \phi(\lambda;p) = \phi_0(\lambda) + \sum_{\mathrm{m}=1}^{\infty} \phi_{\mathrm{m}}(\lambda)p^m \tag{24}$$

in which h_1, h_2, h_3, and h_4 are chosen in such a way that the series (24) are convergent [24] at $p = 1$. Therefore, we have from Eq. (19) that

$$f(\lambda) = f_0(\lambda) + \sum_{\mathrm{m}=1}^{\infty} f_{\mathrm{m}}(\lambda), \quad g(\lambda) = g_0(\lambda) + \sum_{\mathrm{m}=1}^{\infty} g_{\mathrm{m}}(\lambda),$$
$$\theta(\lambda) = \theta_0(\lambda) + \sum_{\mathrm{m}=1}^{\infty} \theta_{\mathrm{m}}(\lambda), \quad \phi(\lambda) = \phi_0(\lambda) + \sum_{\mathrm{m}=1}^{\infty} \phi_{\mathrm{m}}(\lambda) \tag{25}$$

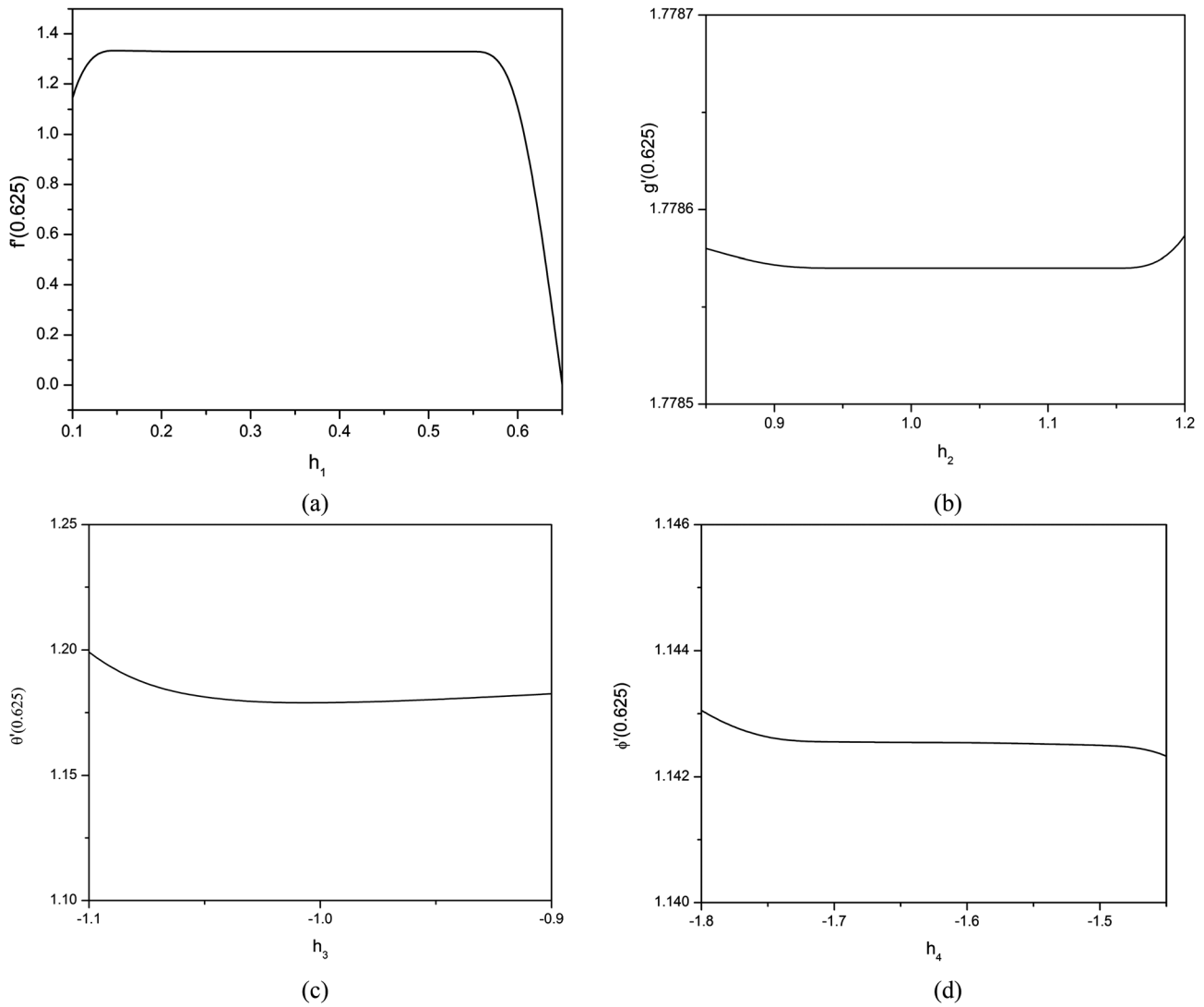

Fig. 1 The *h* curve of (*a*) $f(\eta)$, (*b*) $g(\eta)$, (*c*) $\theta(\eta)$, and (*d*) $\phi(\eta)$

Downloaded from http://asmedigitalcollection.asme.org/heattransfer/article-pdf/135/12/122003/6204608/ht_135_12_122003.pdf by National Institute of Technology- Wamgal user on 08 January 2025

Table 1 Optimal value of h_1 at different order of approximations

Order	Optimal of h_1	Minimum of $E_{f,\mathrm{m}}$
10	0.32	5.73×10^{-7}
15	0.35	2.56×10^{-7}
20	0.35	6.47×10^{-9}

Table 2 Optimal value of h_2 at different order of approximations

Order	Optimal of h_2	Minimum of $E_{g,\mathrm{m}}$
10	1.05	-4.91×10^{-5}
15	1.0	-6.83×10^{-6}
20	1.0	-2.59×10^{-8}

Table 3 Optimal value of h_3 at different order of approximations

Order	Optimal of h_3	Minimum of $E_{\theta,\mathrm{m}}$
10	−0.93	4.90×10^{-5}
15	−0.95	-2.75×10^{-6}
20	−0.95	-6.63×10^{-7}

Table 4 Optimal value of h_4 at different order of approximations

Order	Optimal of h_4	Minimum of $E_{\phi,\mathrm{m}}$
10	−1.55	6.20×10^{-5}
15	−1.6	-4.52×10^{-7}
20	−1.6	-2.81×10^{-7}

where

$$f_{\mathrm{m}}(\lambda) = \frac{1}{m!}\frac{\partial^m f(\lambda;p)}{\partial p^m}\bigg|_{p=0}, \quad g_{\mathrm{m}}(\lambda) = \frac{1}{m!}\frac{\partial^m g(\lambda;p)}{\partial p^m}\bigg|_{p=0},$$

$$\theta_{\mathrm{m}}(\lambda) = \frac{1}{m!}\frac{\partial^m \theta(\lambda;p)}{\partial p^m}\bigg|_{p=0}, \quad \phi_{\mathrm{m}}(\lambda) = \frac{1}{m!}\frac{\partial^m \phi(\lambda;p)}{\partial p^m}\bigg|_{p=0}$$

We presume that the initial guesses to f, g, θ and ϕ the auxiliary linear operators L and the nonzero auxiliary parameters h_1, h_2, h_3, and h_4 are so properly selected that the deformation $f(\lambda,p), g(\lambda,p), \theta(\lambda,p)$, and $\phi(\lambda,p)$ are smooth enough and their mth-order derivatives with respect to p in Eqs. (25) exist. The formulae in Eq. (25) provide us with a direct relationship between the initial guesses and the exact solutions. The convergence of a Taylor series at $p=1$ is a must as proved by Liao [24]. All the effects of micropolar parameter, the heat and mass transfer, chemical reaction parameter, Soret and Dufour effects, velocity and microrotation can be studied from the exact formulae (25).

4 Convergence of the HAM Solution

One of the chief aims of the HAM method is to produce solutions that will converge in a much larger region than the solutions obtained with the traditional methods. Convergence of the solution series depends upon the choice of initial approximations, the

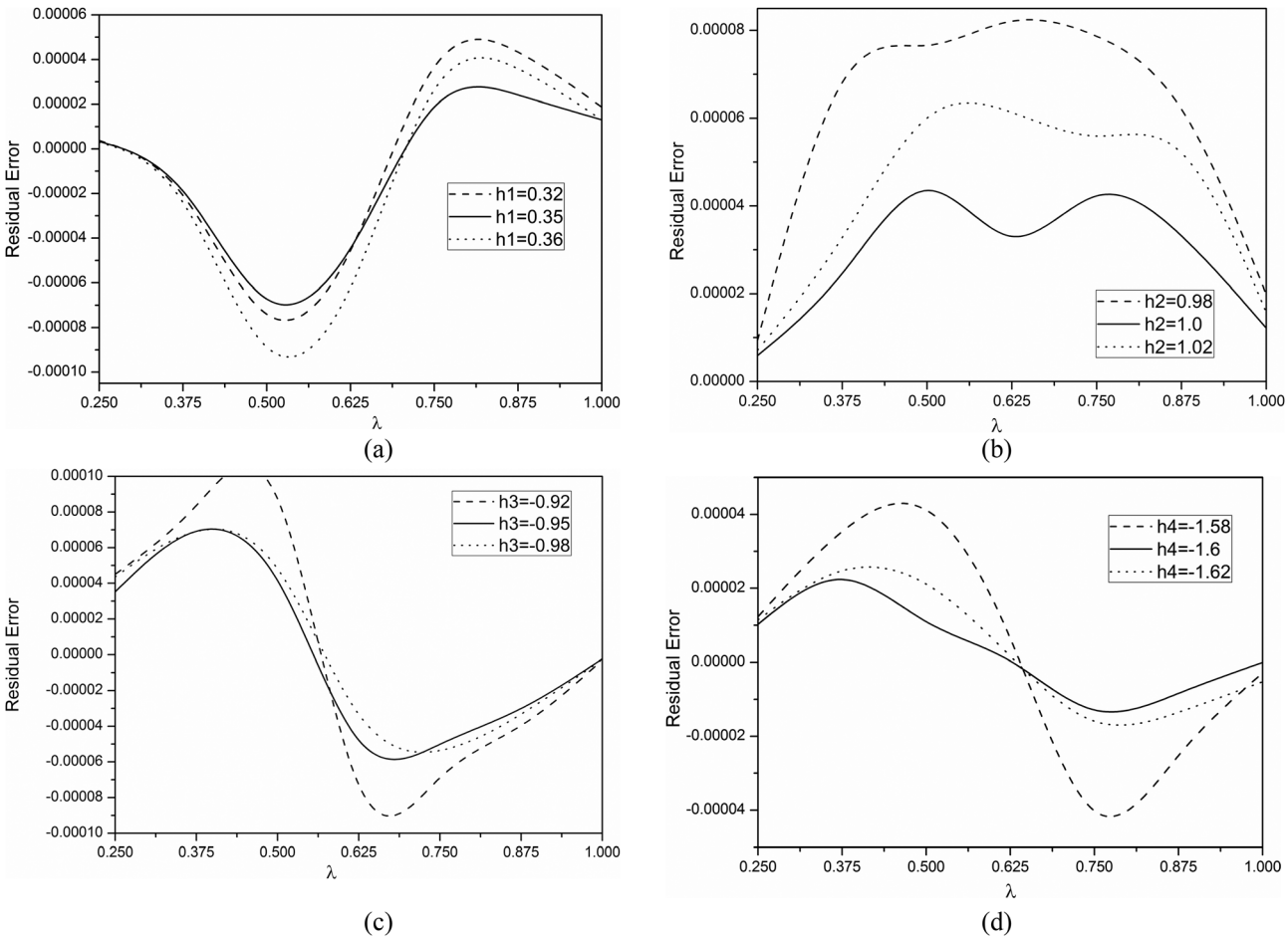

Fig. 2 Residual errors of (*a*) $f(\eta)$, (*b*) $g(\eta)$, (*c*) $\theta(\eta)$, and (*d*) $\phi(\eta)$

Downloaded from http://asmedigitalcollection.asme.org/heattransfer/article-pdf/135/12/122003/6204608/ht_135_12_122003.pdf by National Institute of Technology- Warngal user on 08 January 2025

Table 5 Convergence of HAM solutions for different order of approximations

Order	$f(0.625)$	$g(0.625)$	$\theta(0.625)$	$\phi(0.625)$
5	0.47094772214755665	0.7362762696667875	0.6368498802632638	0.65114803497806615
10	0.47237556807520314	0.7523562797808536	0.6528011865286971	0.66115508567139114
15	0.47252145774545407	0.7523233721746337	0.6528027409476421	0.66115332285792106
20	0.47252143940636366	0.7523231626437272	0.6528027704929337	0.66115331846895047
25	0.47252143940437764	0.7523231610147195	0.6528027702176895	0.66115331828527606
30	0.47252143940416766	0.7523231610137272	0.6528027702129337	0.66115331828489504
35	0.47252143940415764	0.7523231610137197	0.6528027702194755	0.66115331828360475
40	0.47252143940415662	0.7523231610137195	0.6528027702194725	0.66115331828360406

auxiliary linear operators and the nonzero auxiliary parameters. By varying these parameters we can adjust the region in which the series is convergent and the rate at which the series converges. One of the chief factors that influence the convergence of the solution series is the auxiliary parameters h_1, h_2, h_3, and h_4 as pointed by Liao [22]. For this purpose, the h-curves are plotted by choosing h_1, h_2, h_3, and h_4 in such a manner that the solutions (24) ensure convergence Liao [24]. Here to see the admissible values of h_1, h_2, h_3, and h_4 the h-curves are plotted for 20th-order of approximation in Fig. 1 by taking the values of the parameters $gs = 1$; $gc = 0.1$; $Sc = 0.22$; $D_f = 0.03$; $S_r = 2.0$; $K = 0.5$; $N = 0.5$; $m = 2.0$; $H_a = 2$; $\Pr = 0.71$; $\mathrm{Br} = 0.01$; and $B1 = 0.5$. It is clearly noted from Fig. 1 that the range for the admissible values of h_1 is $0.2 < h_1 < 0.5$, h_2 in a region $0.85 < h_2 < 1.15$, the admissible values of h_3 and h_4 are shown in a region $-1.05 < h_3 < -0.85$ and $-1.7 < h_4 < -1.5$. A wide valid zone is evident in these figures ensuring convergence of the series. To choose optimal value of auxiliary parameter, the average residual errors (see Ref. [24] for more details) are defined as

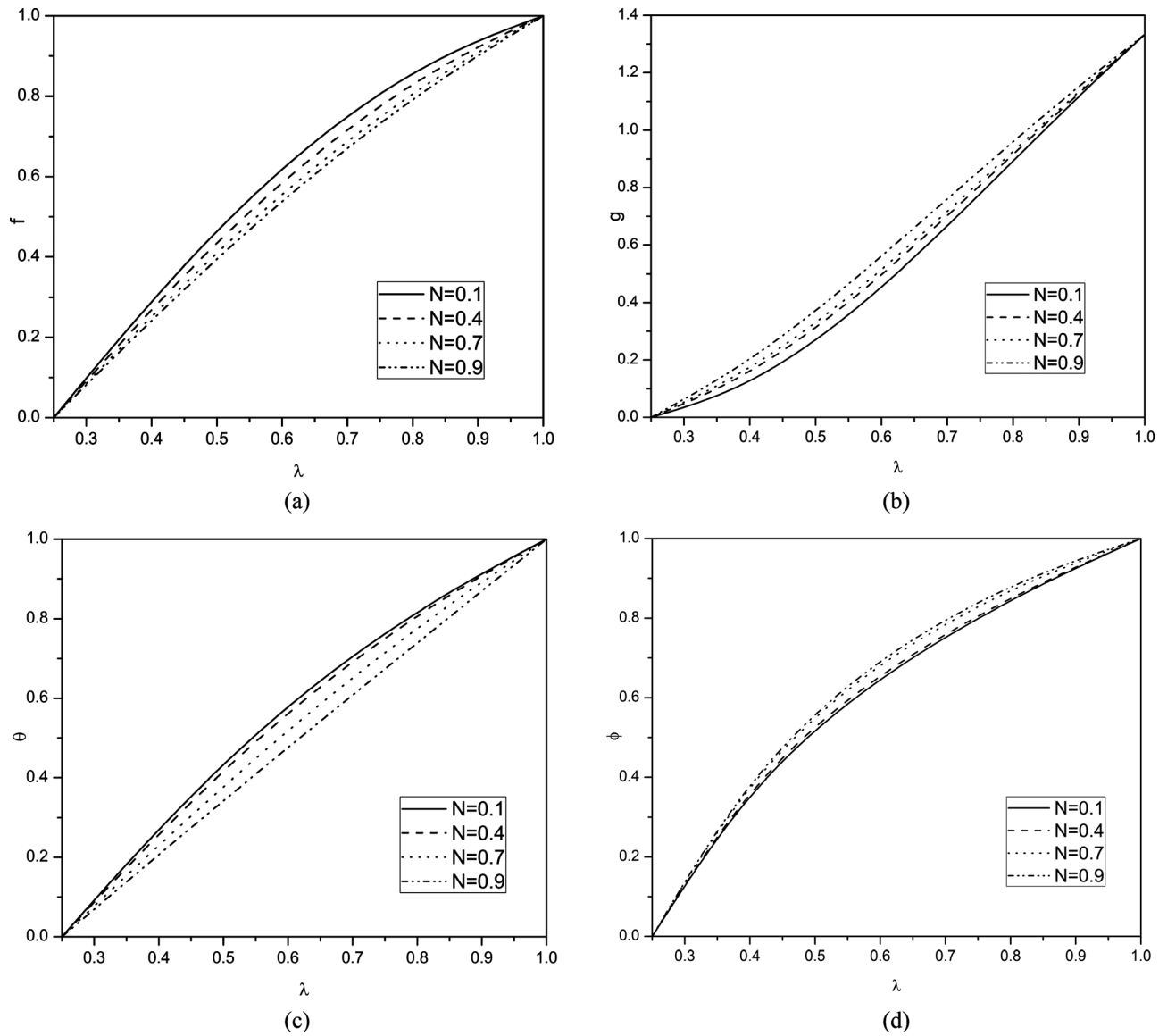

Fig. 3 Effect of coupling numbers on (*a*) velocity(f) (*b*) microrotation (*c*) temperature and (*d*) concentration for $Ha = 3$, $D_f = 0.03$, $S_r = 2$, $K = 0.5$

Downloaded from http://asmedigitalcollection.asme.org/heattransfer/article-pdf/135/12/122003/6204608/ht_135_12_122003.pdf by National Institute of Technology- Warngal user on 08 January 2025

$$E_{f,m} = \frac{1}{K}\sum_{i=1}^{K}\left(N_1\left[\sum_{j=0}^{m} f_j(i\Delta t)\right]\right)^2 \quad (26a)$$

$$E_{g,m} = \frac{1}{K}\sum_{i=1}^{K}\left(N_2\left[\sum_{j=0}^{m} g_j(i\Delta t)\right]\right)^2 \quad (26b)$$

$$E_{\theta,m} = \frac{1}{K}\sum_{i=1}^{K}\left(N_3\left[\sum_{j=0}^{m} \theta_j(i\Delta t)\right]\right)^2 \quad (26c)$$

$$E_{\phi,m} = \frac{1}{K}\sum_{i=1}^{K}\left(N_4\left[\sum_{j=0}^{m} \phi_j(i\Delta t)\right]\right)^2 \quad (26d)$$

where $\Delta t = 1/K$ and $K = 4$. At different order of approximations (m), minimum of average residual errors are shown in Tables 1–4. From these tables, it is found that they are minimum at $h_1 = 0.35, h_2 = 1.0, h_3 = -0.95, h_4 = -1.6$, respectively. Therefore, the optimum values of convergence control parameters are taken as $h_1 = 0.35$, and $h_2 = 1.0, h_3 = -0.95, h_4 = -1.6$.

To see the accuracy of the solutions, the residual errors are defined for the system as

$$\mathrm{RE_f} = -\frac{2N}{1-N}\lambda g_{n'} + \frac{4}{1-N}f_n'' + \sqrt{\lambda}(g_s\theta_n + g_c\phi_n) - H_a^2 f_n \quad (27a)$$

$$\mathrm{RE_g} = -g_n + f_n' + \frac{2(2-N)}{m^2}(g' + \lambda g_n'') \quad (27b)$$

$$\mathrm{RE}_\theta = (\lambda^3\theta_n'' + \lambda^2\theta_n') + \frac{\mathrm{Br}}{1-N} \times \left[(N/2)\lambda^2(f_n' - g_n)^2 + (f_n - \lambda f_n')^2 + \frac{N(2-N)}{m^2}\lambda^3 g_n'^2\right] + D_f P_r(\lambda^3\phi_n'' + \lambda^2\phi_n') \quad (27c)$$

$$\mathrm{RE}_\phi = \frac{1}{S_c}(\lambda\phi_n'' + \phi_n') + S_r(\lambda\theta_n'' + \theta_n') - \frac{K}{4}\phi_n \quad (27d)$$

where $f_n(\lambda), g_n(\lambda)$. $\theta_n(\lambda)$ and $\phi_n(\lambda)$ are the HAM solution for $f(\lambda), \omega(\lambda), \theta(\lambda)$ and $\phi(\lambda)$. For optimality of the convergence control parameters, residual error [25] for different values of h in the convergence region displayed in Figs. 2(*a*)–2(*d*). We examine that

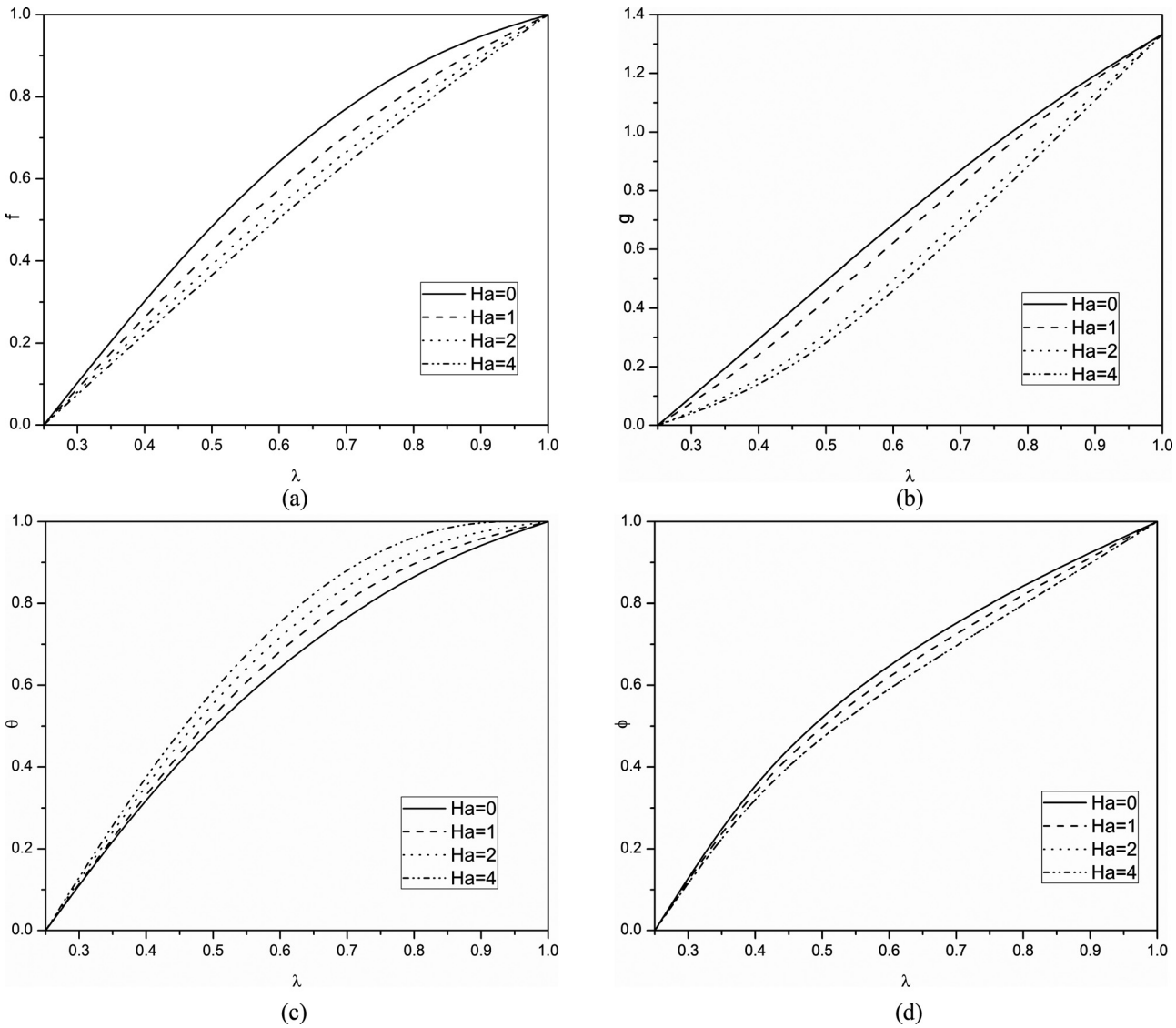

Fig. 4 Effect of Hartman number on (*a*) velocity(f) (*b*) microrotation (*c*) temperature and (*d*) concentration for $N = 0.5$, $D_f = 0.03$, $S_r = 2$, $K = 0.5$

Downloaded from http://asmedigitalcollection.asme.org/heattransfer/article-pdf/135/12/122003/6204608/ht_135_12_122003.pdf by National Institute of Technology- Wamgal user on 08 January 2025

$h_1 = 0.35, h_2 = 1.0, h_3 = -0.95$, and $h_4 = -1.6$ gives a better solution. Table 5 establishes the convergence of the obtained series solution. It is found from the above observations that the series given by Eq. (24) converge in the whole region of λ when $h_1 = 0.35, h_2 = 1.0, h_3 = -0.95$, and $h_4 = -1.6$.

5 Results and Discussion

The system of nonlinear ordinary differential equations (9)–(12) together with the boundary conditions (13) are locally similar and solved analytically using HAM. To have a better understanding of the flow characteristics, velocity, microrotation, temperature and concentration are calculated for the parameters coupling, Hartman number, Dufour, Soret numbers and chemical reaction parameters.

In Figs. 3(*a*)–3(*d*), the effects of coupling number N on the dimensionless velocity, microrotation, temperature and concentration are presented for fixed values of other parameters. The coupling number N characterizes the coupling of linear and rotational motion arising from the micromotion of the fluid molecules. Hence, N signifies the coupling between the Newtonian and rotational viscosities. As $N \to 1$, the effect of microstructure becomes significant, whereas with a small value of N the individuality of the substructure is much less pronounced. As $\kappa \to 0$, i.e., $N \to 0$, the micropolarity is lost and the fluid behaves as nonpolar fluid. Hence, $N \to 0$ corresponds to viscous fluid. As N increases, it is observed from Fig. 3(*a*) that velocity decreases. The velocity in case of micropolar fluid is less compared to that of viscous fluid case ($N \to 0$ corresponds to viscous fluid). Figure 3(*b*) depicts that increasing coupling number increase the microrotation. From Fig. 3(*c*), it is seen that, temperature decreases with increase in the coupling number. An increase in the micropolarity behaves like a cooling agent, a feature which is useful for many real situations. It can be seen from Fig. 3(*d*) concentration of the fluid increases with increase of coupling number.

The variation of the nondimensional velocity, microrotation, temperature and concentration profiles with λ for different values of magnetic parameter is illustrated in Figs. 4(*a*)–4(*d*). It is observed from Fig. 4(*a*) that velocity decreases as the magnetic parameter (H_a) increases. This is due to the fact that the introduction of a transverse magnetic field, normal to the flow direction, has a tendency to create the drag known as the Lorentz force which tends to resist the flow. Hence, the horizontal velocity profiles decrease as the magnetic parameter H_a increases. From

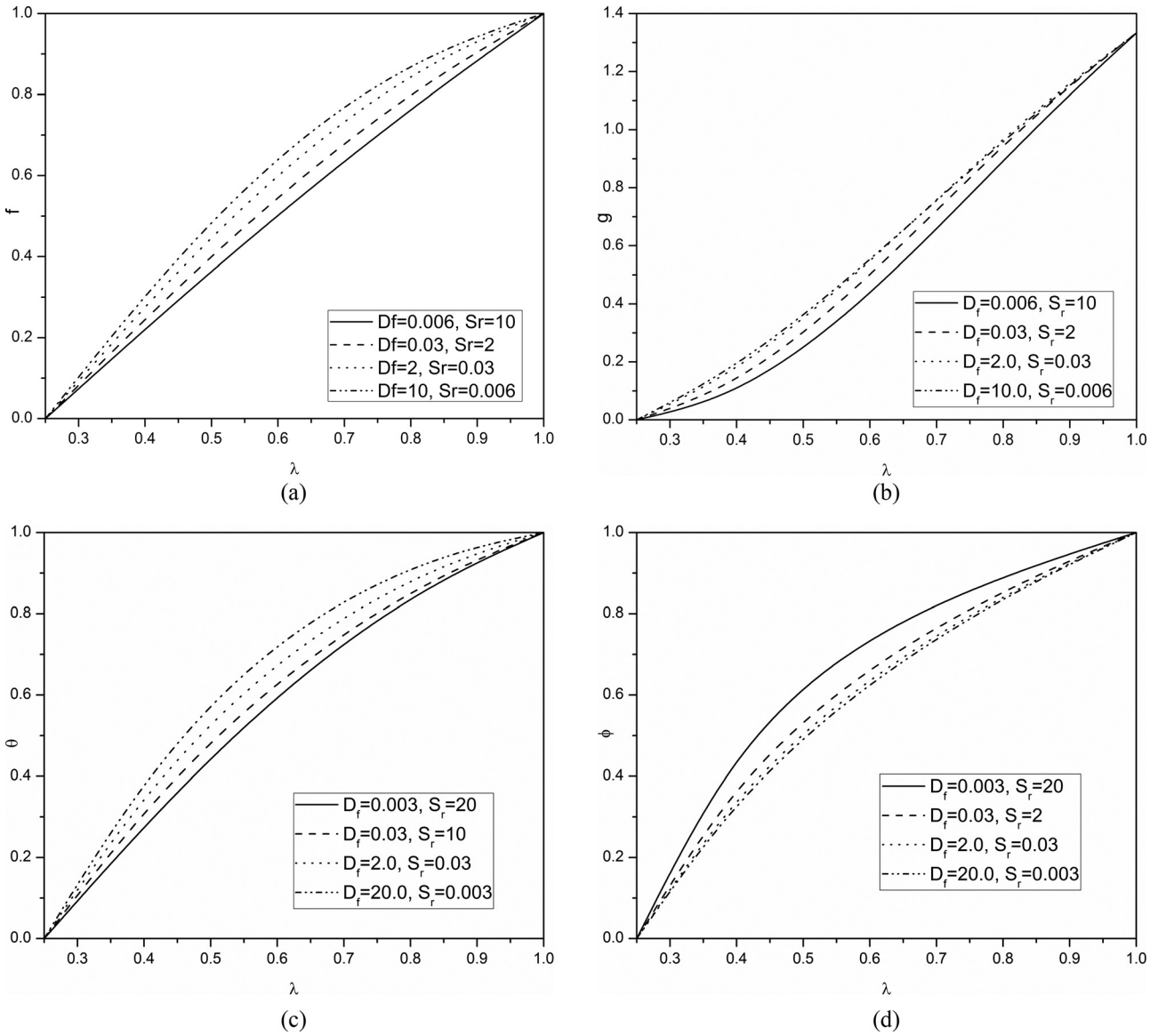

Fig. 5 Effect of Dufour and Soret numbers on (*a*) velocity(f) (*b*) microrotation (*c*) temperature and (*d*) concentration for *Ha* = 3, *N* = 0.5, *K* = 0.5

Downloaded from http://asmedigitalcollection.asme.org/heattransfer/article-pdf/135/12/122003/6204608/ht_135_12_122003.pdf by National Institute of Technology- Warngal user on 08 January 2025

Fig. 4(*b*), it is clear that the microrotation component decreases for increasing values of H_a. It is noticed from Fig. 4(*c*) that the nondimensional fluid temperature increases with increasing values of magnetic parameter. It is clear from Fig. 4(*d*) that the nondimensional fluid concentration decreases with increasing values of H_a. As explained above, the transverse magnetic field gives rise to a resistive force known as the Lorentz force of an electrically conducting fluid. This force makes the fluid experience a resistance by increasing the friction between its layers and thus increases its temperature and concentration.

The effects of Soret and Dufour number on the dimensionless velocity, microrotation, temperature and concentration for fixed values of N, H_a, and K is shown in Figs. 5(*a*)–5(*d*). Majority of the papers that appears in the literature on Dufour and Soret effects on convective flows do not offer a physical basis to calculate Dufour and Soret coefficients [30]. But, Benano-Melly et al. [31], while analyzing the problem of thermal diffusion in binary fluid mixtures, lying within a porous medium and subjected to a horizontal thermal gradient, presented list of references on the measurements and the Dufour coefficient. In the present analysis the values of Soret number S_r and Dufour number D_f are chosen in such a way that their product is a constant 0.06 according to their definition provided that the mean temperature T_m is kept constant [11,32,30]. As Dufour number increases (Soret number decreases), it is seen from Fig. 5(*a*) that the velocity increases. In Fig. 5(*c*), it is observed that the microrotation increases with an increase in Dufour number. Figure 4(*d*) indicates an increase in Dufour number (decrease in Soret number) increases the temperature of the fluid. It is noted from Fig. 5(*d*) that increase in D_f decreases the concentration. The Dufour number denotes the contribution of the concentration gradients to the thermal energy flux in the flow. It can be seen that an increase in the Dufour number causes a rise in the velocity and temperature and a drop in the concentration.

Figures 6(*a*)–6(*d*) represent the effect of chemical reaction K on dimensionless velocity, microrotation, temperature and concentration. It can be seen from these figures that the velocity decreases with an increase in the parameter K. The dimensionless microrotation decreases and temperature increases as K increases. The concentration decreases with an increase in the parameter K. Higher values of K amount to a fall in the chemical molecular diffusivity, i.e., less diffusion. Therefore, they are obtained by species transfer. An increase in K will suppress species concentration. The concentration distribution decreases at all points of the flow field with

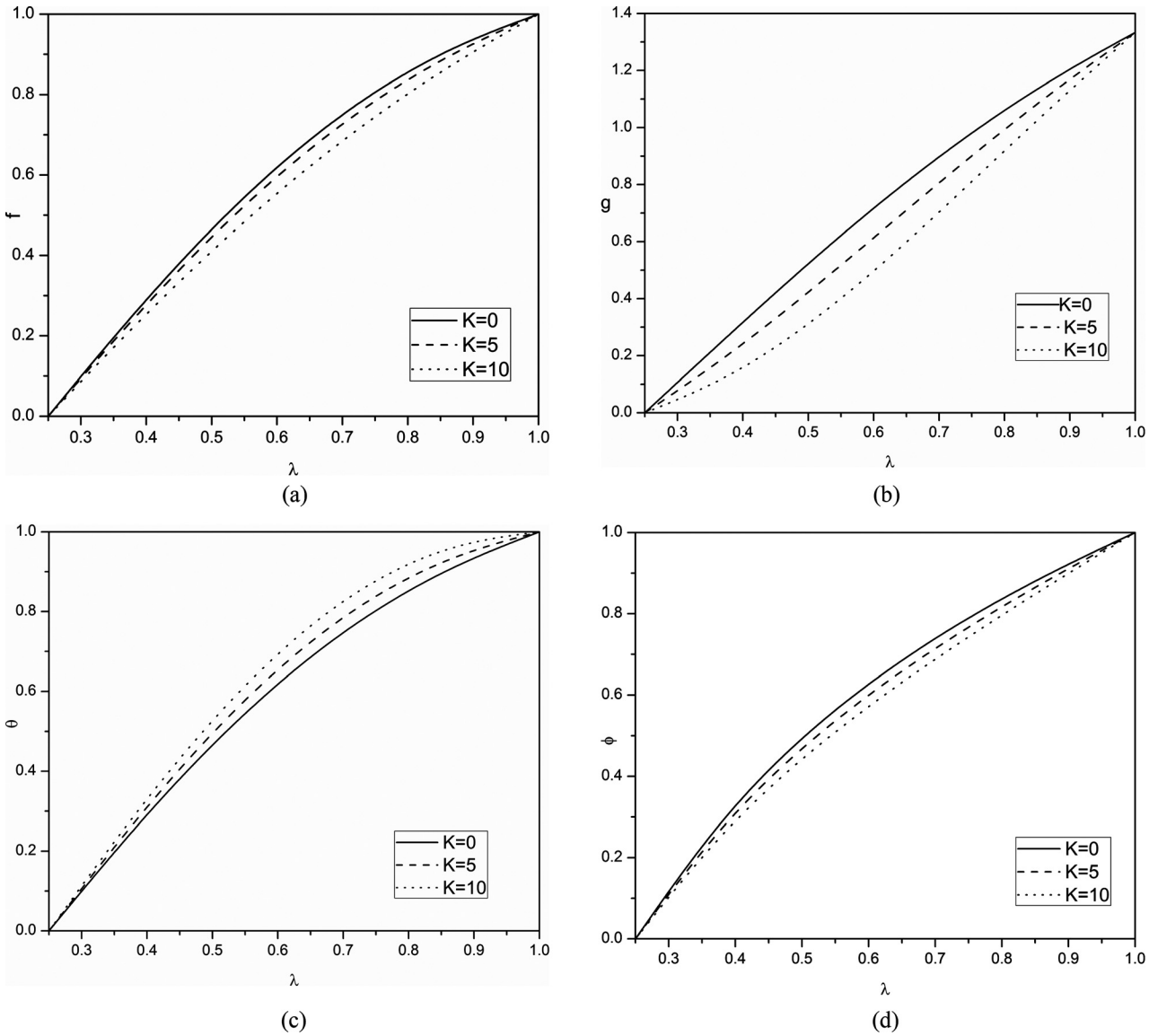

Fig. 6 Effect of chemical reaction parameter on (*a*) velocity(f) (*b*) microrotation (*c*) temperature and (*d*) concentration for $Ha = 3$, $D_f = 0.03$, $S_r = 2$, $N = 0.5$

Downloaded from http://asmedigitalcollection.asme.org/heattransfer/article-pdf/135/12/122003/6204608/ht_135_12_122003.pdf by National Institute of Technology- Warngal user on 08 January 2025

the increase in the reaction parameter. This shows that heavier diffusing species have greater retarding effect on the concentration distribution of the flow field.

6 Conclusions

In this paper, the magnetic, chemical reaction, Dufour and Soret effects on steady flow of a micropolar fluid between concentric annulus with heat and mass transfer has been studied. For the governing systems nonlinear differential equations an approximate analytical series solutions are obtained applying HAM. From the present study we observe that

(1) the larger values of N (i.e., when the microstructure is significant) the velocity and temperature of the fluid decreases where as the concentration increases.
(2) the velocity, microrotation and concentration decreases with an increase in the magnetic parameter.
(3) the velocity, microrotation and the dimensionless temperature of the fluid increases with the increase of Dufour number (or decrease of Soret number) and with increase of Dufour number (or decrease of Soret number) the concentration of the fluid decreases.
(4) the velocity, microrotation and concentration decreases with the increase in the reaction parameter.

Nomenclature

B_r = Brinkman number
C = concentration
C_p = specific heat at constant pressure
C_s = concentration susceptibility
S = couple stress parameter
D_f = Dufour number
D_m = mass diffusivity
f = dimensionless stream function
g = acceleration due to gravity
Gr_C = mass Grashof number
Gr_T = temperature Grashof number
k_1 = rate of chemical reaction
K = chemical reaction parameter
K_T = thermal diffusion ratio
Pr = Prandtl number
Re = Reynolds number
Sc = Schmidt number
S_r = Soret number
T = temperature
T_m = mean fluid temperature
u = velocity components in the direction of φ

Greek Symbols

η = similarity variable
η_1 = the coupling material constant
α = thermal diffusivity
β_T = coefficient of thermal expansion
β_c = coefficient of concentration expansion
ρ = density of the fluid
ν = kinematic viscosity
θ = dimensionless temperature
ϕ = dimensionless concentration
μ = viscosity of the fluid

Superscript

$'$ = differentiation with respect to λ

References

[1] Aung, W., Kakac, S., and Shah, R. K., 1987, *Handbook of Single-Phase Convective Heat Transfer*, Wiley, New York, Chap. 15.
[2] Jackson, J. D., Cotton, M. A., and Axcell, B. P., 1989, "Studies of Mixed Convection in Vertical Tubes," Int. J. Heat Fluid Flow, **10**, pp. 2–15.
[3] Taylor G. I., 1923, "Stability of a Viscous Liquid Contained Between Two Rotating Cylinders," Philos. Trans. R. Soc. London, Ser. A, **223**, pp. 289–343.
[4] Fusegi T., Farouk B., and Ball K. S., 1986, "Mixed-Convection Flows Within a Horizontal Concentric Annulus With a Heated Rotating Inner Cylinder," Numer. Heat Transfer, **9**, pp. 591–604.
[5] Kataoka K., 1986, "Taylor Vortices and Instabilities in Circular Couette Flows," *Encyclopaedia of Fluid Mechanics*, N. P. Cheremisinoff, ed., Gulf, Houston, TX.
[6] El-Shaarawi M. A. I., and Khamis M., 1987, "Induced Flow in Uniformly Heated Vertical Annuli With Rotating Inner Walls," Numer. Heat Transfer, **12**, pp. 493–508.
[7] Kou, H. S., and Huang, D. K., 1997, "Fully Developed Laminar Mixed Convection Through a Vertical Annular Duct Filled With Porous Media," Int. Commun. Heat Mass Transfer, **24**(1), pp. 99–110.
[8] Kermlt L. Holman, Sudhir. T. Ashar, 1971, "Mass Transfer in Concentric Rotating Cylinders With Surface Chemical Reaction in the Presence of Taylor Vortexes," Chem. Eng. Sci., **26**, pp. 1817–1831.
[9] Pop, I., Grosan, T., and Cornelia, R., 2010, "Effect of Heat Generated by an Exothermic Reaction on the Fully Developed Mixed Convection Flow in a Vertical Channel," Commun. Nonlinear Sci. Numer. Simul., **15**, pp. 471–474.
[10] Shateyi, S., Motsa, S. S., and Sibanda, P., 2010, "Homotopy Analysis of Heat and Mass Transfer Boundary Layer Flow Through a Non-Porous Channel With Chemical Reaction and Heat Generation," Can. J. of Chem. Engg., **88**, pp. 975–982.
[11] Kafoussias N. G., and Williams E. W., 1995, "Thermal-Diffusion and Diffusion-Thermo Effects on Mixed Freeforced Convective and Mass Transfer Boundary Layer Flow With Temperature Dependent Viscosity," Int. J. Eng. Sci., **33**(9), pp. 1369–1384.
[12] Awad F., and Sibanda P.,2010, "Dufour and Soret Effects on Heat and Mass Transfer in a Micropolar Fluid in a Horizontal Channel," WSEAS Trans. Heat Mass Transfer, **5**, pp. 165–177.
[13] Sudarsan Reddy, P., Prasada Rao, D. R. V., Mamatha, E., and Srinivas, G., 2010, "Finite Element Analysis of Thermo-Diffusion and Diffusion-Thermo Effects on Convective Heat and Mass Transfer Flow Through a Porous Medium in Cylindrical Annulus in the Presence of Constant Heat Source," Int. J. Appl. Math Mech., **6**(7), pp. 43–62.
[14] Sulochana, C., Gururaj, N., and Devika, S., 2011, "Finite Element Analysis of Thermo-Diffusion Effect on Convective Heat and Mass Transfer Through a Porous Medium in Circular Annulus," Int. J. Appl. Math Mech., **7**(6), pp. 80–101.
[15] Takhar, H. S., Ali, M. A., and Soundalgekar, V. M., 1989, "Stability of MHD Couette Flow in a Narrow Gap Annulus," Appl. Sci. Res., **46**, pp. 1–24.
[16] Panja, S., Sengupta, P. R., and Debnath, L., 1996, "Hydromagnetic Flow of Reiner-Rivlin Fluid Between Two Coaxial Circular Cylinders With Porous Walls," Comput. Math. Appl., **32**(2), pp. 1–4.
[17] KunugiLi, F. C. T., and Serizawa, A., 2005, "MHD effect on Flow Structures and Heat Transfer Characteristics of Liquid Metal-Gas Annular Flow in a Vertical Pipe," Int. J. Heat Mass Transfer, **48**, pp. 2571–2581.
[18] Siddiqa, S., Hossain, Md. A., Suvash, C. S., 2012, "Double Diffusive Magneto-Convection Fluid Flow in a Strong Cross Magnetic Field With Uniform Surface Heat and Mass Flux," ASME J. Heat Transfer, **134**(11), p.114506.
[19] Ericksen, J. C., 1960, "Anisotropic Fluids," Arch. Ration. Mech. Anal. **4**, pp. 231–237.
[20] Ericksen, J. C., 1960 "Transversely Isotropic Fluids," Colloid Polym. Sci, **173**, pp. 117–122.
[21] Eringen, A. C., 1966, "Theory of Micropolar Fluids," J. Math. Mech. **16**, pp. 1–18.
[22] Liao, S. J., 2003, *Beyond Perturbation. Introduction to Homotopy Analysis Method*, Chapman and Hall/CRC Press, Boca Raton, FL.
[23] Liao, S. J., 2004, "On the Homotopy Analysis Method for Nonlinear Problems," Appl. Math. Comput., **147**(2), pp. 499–513.
[24] Liao, S. J., 2010, "An Optimal Homotopy-Analysis Approach for Strongly Nonlinear Differential Equations," Commun. Nonlinear Sci. Numer. Simul., **15**, pp. 2003–2016.
[25] Rashidi, M. M., Mohimanian pour, S. A., Abbasbandy, S., 2011, "Analytic Approximate Solutions for Heat Transfer of a Micropolar Fluid Through a Porous Medium With Radiation," Commun. Nonlinear Sci. Numer. Simul., **16**, pp. 1874–1889.
[26] Si, X.-H., Zheng, L.-C., Zhang, X.-X., and Chao, Y., 2011, "Homotopy Analysis Solutions for the Asymmetric Laminar Flow in a Porous Channel With Expanding or Contracting Walls," Acta Mech. Sin., **27**(2), pp. 208–214.
[27] Kazakia, Y., and Ariman, T.,1971, "Heat-Conducting Micropolar Fluids," Rheol. Acta, **10**, pp. 319–325.
[28] Ramkzssoon, H., and Majumdar, S. R., 1977, "Unsteady Flow of a Micropolar Fluid Between Two Concentric Circular Cylinders," Can. J Chem Eng., **55**, pp. 408–413.
[29] van Gorder, R.A., and Vajravelu, K., 2009, "On the Selection of Auxiliary Functions, Operators, and Convergence Control Parameters in the Application of the Homotopy Analysis Method to Nonlinear Differential Equations: A General Approach," Commun. Nonlinear Sci. Numer. Simul., **14**, pp. 4078–4089.
[30] Postelnicu, A., 2010, "Heat and Mass Transfer by Natural Convection at a Stagnation Point in a Porous Medium Considering Soret and Dufour Effects," Heat Mass Transfer, **46**, pp. 831–840.
[31] Benano-Melly, L. B., Caltagirone, J. P., Faissat, B., Montel, F., and Costeseque, P., 2001,"Modelling Soret Coefficient Measurement Experiments in Porous Media Considering Thermal and Solutal Convection," Int. J. Heat Mass Transfer, **44**, pp. 1285–1297.
[32] Anghel, M., Takhar, H. S., and Pop, I., 2000, "Dufour and Soret Effects on Free Convection Boundary-Layer Over a Vertical Surface Embedded in a Porous Medium," Studia Universitatis Babes-Bolyai, Mathematica, **XLV**, pp. 11–22.

Downloaded from http://asmedigitalcollection.asme.org/heattransfer/article-pdf/135/12/122003/6204608/ht_135_12_122003.pdf by National Institute of Technology- Wamgal user on 08 January 2025